High-homogeneity functional parcellation of human brain for investigating robust functional connectivity

Xiangyu Liu, Hua Xie, Brian Nutter, Sunanda Mitra
Dept. of Electrical and Computer Engineering
Texas Tech University
Lubbock, Texas
sunanda.mitra@ttu.edu

***Abstract*—Over the years, resting state functional magnetic resonance imaging (rsfMRI) has been a preferred design tool to analyze human brain functions and brain parcellations. Several different statistical methods have been proposed to study functional connectivity and generate various parcellation atlases based on corresponding connectivity maps. In this study, we employ a sliding window correlation method to generate accurate individual voxel-wise dynamic functional connectivity maps, based on which the brain can be parcellated into highly homogeneous functional parcels. Because there is no ground truth for functional brain parcellation, we accomplish parcellation via k-means clustering to compare with other available parcellations. With temporal characteristics of functional connectivity taken into consideration, high homogeneity can be observed in high resolution parcellation of human brain.**

Keywords-rsfMRI; Human brain; functional connectivity; parcellation; homogeneity

I. INTRODUCTION

Significant progress has been made recently in exploring the neuroimaging field with growing brain imaging technologies [1]. Magnetic resonance imaging (MRI) as well as functional magnetic resonance imaging (fMRI), electroencephalography (EEG), and other widely applied modalities contribute to the blossoming of neuroimaging studies inquiring the structure and function of neural system related to cognitive or behavioral activity. Functional magnetic resonance imaging, a noninvasive measure of blood oxygenation level dependent (BOLD) changes to map neural activity, played an important role in studying neural mechanisms in the human brain over the past few decades [2]. Based on resting state fMRI (rsfMRI) measuring spontaneous fMRI data without active tasks [3][4], a complex neural network comprised of neuronal interconnections can be estimated to infer functional connectivity between different brain areas [5] and explore the large-scale functional organization of brain systems [6] to further examine a disease or disorder. Defining the regions of interests is essential for functional connectivity modeling [7]. Several anatomical or functional atlases have been proposed, e.g. Automated Anatomical Labelling (AAL) and Brodmann's interactive atlases, to provide a set of regions of interest (ROI), but they tend to be mutually discordant and not comprehensively suitable for various data [8]. Therefore, a few brain parcellation approaches, generally, with functional connectivity (FC) based upon temporal or spatial information combining with some clustering methods, have been developed to derive meaningful ROIs and reflect the properties of whole-brain connectome [9]. Dynamic FC (dFC) which quantifies the time-varying inter-regional correlation of segmented time series, may allow us to comprehend the essential configuration of brain networks [10]. dFC characteristics are usually acquired using a sliding window approach, which estimates the time-varying correlation by shifting a fixed window of given samples [11]. With this initiative, voxel-wise dFC clustering is proposed to provide a new insight into accurate brain parcellations with high homogeneity. In this study, the subject brain is functionally subdivided into 50-600 homogeneous parcels via k-means clustering on voxel-wise dFC maps generated by a sliding window approach. This parcellation method is evaluated with specific cluster validity analysis.

Given several disadvantages with the traditional sliding window method, e.g. all observations within the window are weighted equally [12] with inherent variation and spurious fluctuations caused by the arbitrary choice of window length, we investigated dFC using a flexible sliding window approach with adaptive window length selection algorithm proposed in [13] for generation of a voxel-wise dFC map.

II. METHODS

A. Data acquisition

This parcellation is performed on the Cleveland CCF dataset [14], freely available from the 1000 Functional Connectomes Project [15]. In the dataset, a set of six-minute resting state scans were collected from 31 healthy controls (11 males/20 females) on a 3.0T Siemens Trio Tim scanner with repetition time TR = 2800 ms; echo time TE = 29 ms; flip angle = 80°; 31 slices and matrix size = 128 × 128; and acquisition voxel size = 2 × 2 × 4 mm.

B. Preprocessing

fMRI data were preprocessed using an analysis pipeline described in [7] mainly via SPM12 software [16] running in MATLAB 2017b. The first five image volumes were discarded considering the T1 equilibration effects. The preprocessing procedure for all fMRI images is as follows:

realignment with motion correction; normalization with corresponding anatomical images; registration into MNI152 space at 2×2×2 mm^3 resolution; spatially smoothing using an Gaussian kernel with FWHM = 8 mm and finally a band-pass filter restricting the frequency between 0.009 Hz and 0.08 Hz was employed to get rid of artifacts entangled in time courses.

C. Sliding windowed correlation

A general sliding window approach, referred to as fixed dFC in the study, for estimating dFC has been commonly used in the past few years. Given time series $x = (x_1, \cdots, x_N)$ and $y = (y_1, \cdots, y_N)$ from two voxels, the sliding-window covariance and Pearson correlation coefficient can be defined as

$$C_{xy}[n] = \frac{TR}{W}\sum_{n-\Delta}^{n+\Delta}(x_i - \bar{x}_n)(y_i - \bar{y}_n) \quad (1)$$

$$\rho_{xy}[n] = \frac{C_{xy}[n]}{\sqrt{C_{xx}[n]C_{yy}[n]}} \quad (2)$$

respectively, where $w = (2\Delta + 1)TR$ is the window length in seconds and $\bar{x}_n$ is the local average over the window at time point n. In this study, Δ is selected as 8, which means fixed window length is 47.6 secs.

Recently, an adaptive sliding window approach, called adaptive dFC, is introduced in [13] combining local polynomial regression (LPR) and intersection of confidence intervals (ICI) to select an optimal bandwidth to minimize the mean square error (MSE) locally with the assumption that the globally non-stationary processes are stationary locally with infinite samples. The time variant covariance $m(n)$ is estimated by LPR with minimum weighted (windowed) least square error between the approximate polynomials of covariance with coefficient $\beta(n)$ and the inner product $I(n) = x_n y_n$ of two non-stationary processes. Specifically, the goal is to minimize the following cost function at time point n_0,

$$\sum_{n=1}^{N} K_h(n - n_0)\left[x_n y_n - \sum_{k=0}^{p}\beta_k(n_0)(n - n_0)^k\right]^2 \quad (3)$$

where h is a bandwidth controlling the local window size, and K_h is the weighted window function $K_h(n - n_0) = \frac{1}{h}K(\frac{1}{h}(n - n_0))$. Here, $\beta_k(n_0) = \frac{1}{k!}m^{(k)}(n_0)$ is the k^{th} polynomial coefficient. Variable bandwidth h would be investigated for optimal results. As suggested by previous studies, the minimum window length should be larger than $\frac{(p+1)}{(2f)}$, where f is the assumed minimum frequency, while maximum bandwidth equals one half of one block paradigm during acquisition of the task-related fMRI signal. Hence, p would be chosen as 1 for satisfying the rule proposed previously in [17], i.e. $w > \frac{1}{f_{min}}$ for removing lower frequency components. The optimal window is the Epanechnikov kernel, which minimizes the asymptotic MSE of the estimator for such choices of parameters. In this study, the range of bandwidth is given as [47.6 secs, 70 secs].

Next, the optimal bandwidth for each time point is rendered by the ICI method with the maximal window length retaining the intersection of the confidence intervals. These adaptive bandwidths will be employed in the calculation of the Pearson correlation coefficient for more accurate representation of dFC between fMRI time series.

This modified adaptive dFC method has been first applied on synthetic data to rule out the spurious fluctuations in dFC caused by the inherent variation while using fixed dFC leading to smoother correlation timeseries as shown in Fig. 1.

D. Whole brain parcellations on voxel-wise dFC map

The central voxel time course was selected to be correlated with all the other voxel time courses to generate dFC maps via two approaches, adaptive dFC and fixed dFC. Then the k-means clustering [18] is used to minimize the Euclidian distance in parcels for grouping voxels with similar dFC profiles without considering the spatial structure of the brain. Basically, the algorithm proceeds by alternating between two steps: (1) assignment of each dFC time series to the cluster with resulting least sum of squares within it, and (2) update of new centroids in the new clusters. The evaluation of brain parcellation was assessed by clustering, resulting in varying number of parcels (from 50 to 600) with the interval of 50. One cluster validity measure, homogeneity, is employed to examine clustering quality in the study.

E. Homogeneity

One evaluation criteria for a parcellation method is the degree of homogeneity of parcels, which quantifies the average similarity, specifically Pearson correlation coefficients, of pair-wise time courses within the parcels [7] [9] normalized by Fisher's z transformation. The summation of weighted degrees of average parcel homogeneity among the brain produces the subject-level quality indicator of the parcellation algorithm, called global homogeneity:

$$H = \sum_{i=1}^{k}\frac{n_i}{N}\frac{\sum_{u=1}^{n_i-1}\sum_{v=u+1}^{n_i} f(\rho_{uv})}{n_i(n_i-1)/2} \quad (4)$$

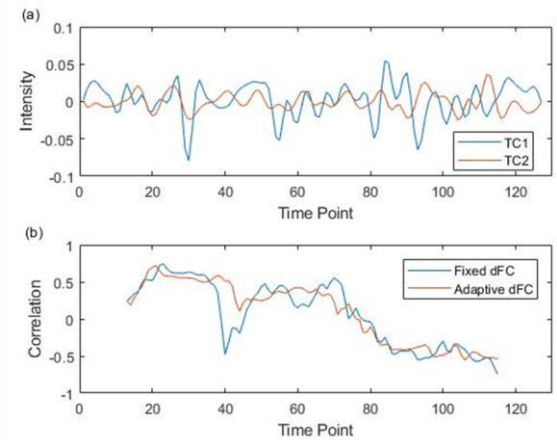

Figure 1. Example of two time courses (a) and corresponding dFCs (b) measured via two sliding window methods.

where k is the number of clusters, n_i is the number of voxels in cluster i and N is the total valid number of voxels within the brain. $f(\rho_{uv})$ represents fisher's z-transformed pair-wise correlation between two different voxels u and v. A favorable parcellation may have a higher global homogeneity value, leading to an accurate description of functional architecture of human brains.

III. Results and Discussion

Multi-resolution parcellation has been performed using two dFC approaches (i.e. fixed and adaptive dFC) with various desired number of ROIs. The color-coded visualization on three anatomical slices of clustering results for number of ROIs equals to 50, 300 and 600 are shown in Fig. 2. Some disconnected clusters are produced by k-means clustering method. The similarity between two sets of parcellation is prominent. Most regions parcellated by the proposed two methods with the same constraints are similar. With smaller number of ROIs, many known brain modules can be revealed [19], such as visual module and motor module. Clustering with larger number of ROIs results in some fine-scale connectivity parcellation with high cluster quality, which may provide some insights in understanding of brain functions in future studies. Fig. 3 presents subject-level homogeneity results averaged across subjects via two approaches. Both approaches achieve relatively high homogeneity compared to many other parcellation reported in [9] and [19], while homogeneities obtained by adaptive dFC is 5%-10% lower than fixed dFC. Although adaptive dFC could remove several spurious fluctuations and capture greater information with large sliding windows, the smoothed correlation series may lead to loss of transient information lowering clustering accuracy.

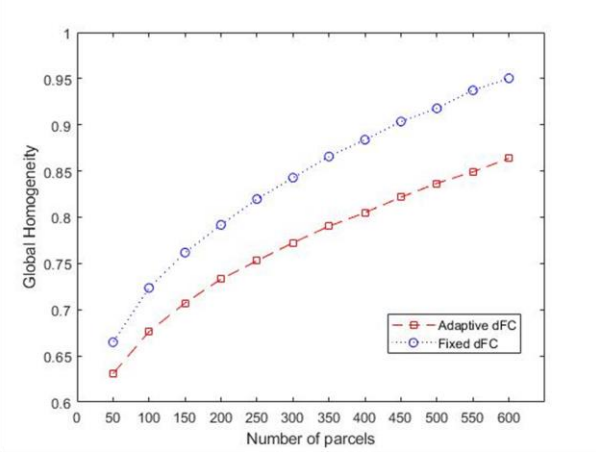

Figure 3. Subject homogeneity averaged across subjects. With increasing parcel number, the homogeneity approaches 1, which shows the superiority of the proposed approach.

IV. Conclusion

Voxel-wise dynamic functional connectivity contributes dramatically to high-homogeneity and high-resolution parcellation. This proposed parcellation with high homogeneity can be conducive to the accuracy of functional connectivity modeling. The fine-scale and coarse-scale parcellations may provide complimentary information on the configuration of functional connectivity network patterns. Furthermore, some other evaluation measures can be investigated in future work validating the proposed approaches.

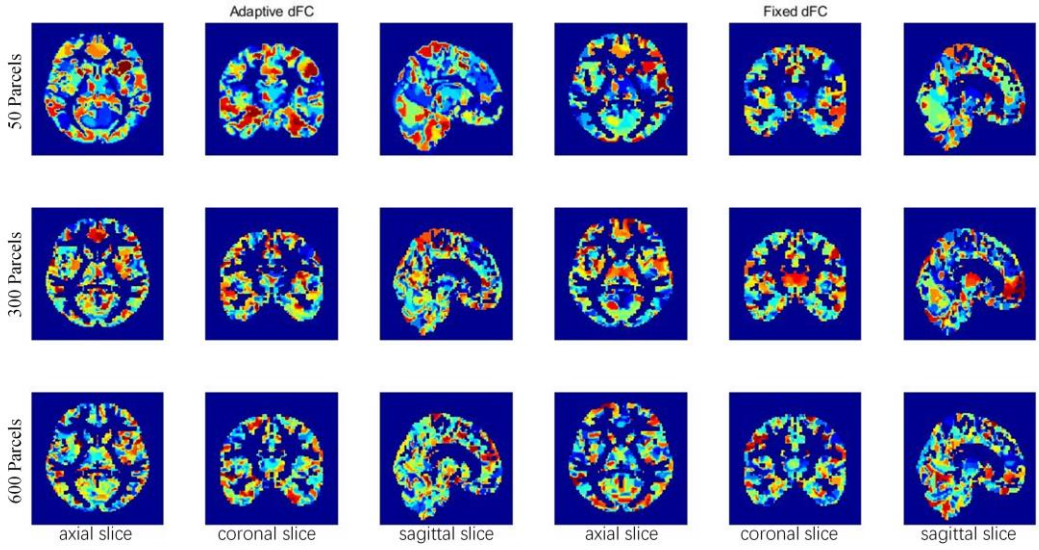

Figure 2. Illustration of parcellation with 50, 300 and 600 parcels in MNI space (x = 9 mm, y = -12mm, z = 0 mm). Both dFC approaches turn out similar subdivision of brian with some variations, especially with a small amount of parcels. (Note: the colors are randomly assigned)

ACKNOWLEDGMENT

This project was supported by the NLM-NIH contract [HHSN276201 500690P]. We gratefully acknowledge many discussions, evaluations and feedback regarding this research effort with Harshit Parmar and Omid Bazgir.

REFERENCES

[1] Bowman, F. DuBois. "Brain imaging analysis." Annual review of statistics and its application 1 (2014): 61-85.

[2] Huettel, Scott A., Allen W. Song, and Gregory McCarthy. Functional magnetic resonance imaging. Sunderland: Sinauer Associates, 2004.

[3] Biswal, Bharat, et al. "Functional connectivity in the motor cortex of resting human brain using echo-planar mri." Magnetic resonance in medicine 34.4 (1995): 537-541.

[4] Smith, Stephen M., et al. "Resting-state fMRI in the human connectome project." Neuroimage 80 (2013): 144-168.

[5] Sporns, Olaf. "The human connectome: a complex network." Annals of the New York Academy of Sciences 1224.1 (2011): 109-125.

[6] Bullmore, Ed, and Olaf Sporns. "Complex brain networks: graph theoretical analysis of structural and functional systems." Nature Reviews Neuroscience 10.3 (2009): 186-198.

[7] Craddock, R. Cameron, et al. "A whole brain fMRI atlas generated via spatially constrained spectral clustering." Human brain mapping 33.8 (2012): 1914-1928.

[8] Thirion, Bertrand, et al. "Which fMRI clustering gives good brain parcellations?." Frontiers in neuroscience 8 (2014).

[9] Arslan, Salim, et al. "Human Brain Mapping: A Systematic Comparison of Parcellation Methods for the Human Cerebral Cortex." NeuroImage (2017).

[10] Xie, Hua, et al. "Whole-brain connectivity dynamics reflect both task-specific and individual-specific modulation: a multitask study." NeuroImage (2017).

[11] Hutchison, R. Matthew, et al. "Dynamic functional connectivity: promise, issues, and interpretations." Neuroimage 80 (2013): 360-378.

[12] Lindquist, Martin A., et al. "Evaluating dynamic bivariate correlations in resting-state fMRI: a comparison study and a new approach." Neuroimage 101 (2014): 531-546.

[13] Fu, Zening, et al. "Adaptive covariance estimation of non-stationary processes and its application to infer dynamic connectivity from fMRI." IEEE transactions on biomedical circuits and systems 8.2 (2014): 228-239.

[14] Lowe, Mark J., et al. "Resting state sensorimotor functional connectivity in multiple sclerosis inversely correlates with transcallosal motor pathway transverse diffusivity." Human brain mapping 29.7 (2008): 818-827.

[15] Biswal, Bharat B., et al. "Toward discovery science of human brain function." Proceedings of the National Academy of Sciences 107.10 (2010): 4734-4739.

[16] Friston, Karl J., et al. "Statistical parametric maps in functional imaging: a general linear approach." Human brain mapping 2.4 (1994): 189-210.

[17] Leonardi, Nora, and Dimitri Van De Ville. "On spurious and real fluctuations of dynamic functional connectivity during rest." Neuroimage 104 (2015): 430-436.

[18] Hartigan, John A., and Manchek A. Wong. "Algorithm AS 136: A k-means clustering algorithm." Journal of the Royal Statistical Society. Series C (Applied Statistics) 28.1 (1979): 100-108.

[19] Gordon, Evan M., et al. "Generation and evaluation of a cortical area parcellation from resting-state correlations." Cerebral cortex 26.1 (2014): 288-303.